EUROPEAN COMMISSION

Community research

EURATOM

Long-term Performance of Engineered Barrier Systems

PEBS

Long-term Performance of Engineered Barrier Systems

PEBS

DELIVERABLE (D-N^{O}:DB-WP3)

Comparison of CODE-BRIGHT and LAGAMINE for THM modeling

Authors:

Yuemiao Liu, Ju Wang, Shengfei Cao, Liang Chen

Date of issue of this report:20/11/2013

Start date of project: 01/03/10 Duration: 48 Months

Seventh Euratom Framework Programme for Nuclear Research & Training Activities		
Dissemination Level		
PU	Public	PU
RE	Restricted to a group specified by the partners of the PEBS project	
CO	Confidential, only for partners of the PEBS project	

BRIUG 中核集团核工业北京地质研究院

CNNC Beijing Research Institute of Uranium Geology

CONTENTS

Abstract

In order to investigate the performance of bentonite under THM coupled condition, a series of mock-up facilities were constructed in the laboratory. The conditions of the bentonite in an engineered barrier for high-level radioactive waste disposal were simulated in a series of tests performed in cylindrical cells. A fully coupled thermo-hydro-mechanical (THM) formulation has been adopted as a general framework to analyze these FEBEX experiments by using the software of CODE-BRIGHT. This work presents the comparisons between the variables recorded online during the tests and the model results. The main results of the postmortem analysis are also modeled. Also in this report, another constitutive model is proposed to tackle the principal THM coupling behavior of GMZ bentonite. With the proposed model, numerical simulations of the China-Mock-up test are carried out by using the code of LAGAMINE. A qualitative analysis of the predictive results is carried out, including the variation of temperature, saturation degree, suction and swelling pressure of the compacted bentonite. It is suggested that the proposed model is capable to reproduce the principal physical-mechanical behavior of GMZ bentonite.

KEYWORDS: High-level radioactive waste (HLW), geological repository, bentonite, lab testing, mock-up test, numerical modeling, thermo-hydro-mechanical (THM)

1. Background

Deep geological disposal is internationally recognized as the most feasible and effective way to dispose of high-level radioactive waste (HLW). Repositories are generally designed on the basis of a multiple barrier system concept, which is mainly composed by engineered and natural barriers between the HLW and the biosphere. As the last line of defense between the waste container and host rock, the buffer/backfill is one of the most important components in the engineered barrier system. In the life cycle of the HLW disposal project, the buffer/backfill will be subjected to temperature increase due to heat emitted by the waste and hydration from water coming from the adjacent rocks (Gens et al, 2010). The buffer/backfill material is designed to stabilize the repository excavations and the coupled thermo-hydro-mechanical-chemical (THMC) conditions, and to provide low permeability and long-term retardation (Wang, 2010). A bentonite-based material is often proposed or considered as a possible buffer/backfill material for the isolation of the HLW. To guarantee the long-term safety of the engineered barrier, it is necessary to conduct research on coupled THMC behaviors of bentonite under simulative geological disposal conditions, and subsequently to reveal the property changes of the bentonite over a long period of time.

To understand the complex behaviors of the buffer/backfill material located in the coupled THMC environment, in recent years, there has been an increasing interest internationally in the construction of large-scale mock-up experimental facilities in the laboratory and in situ such as the Long Term Experiment of Buffer Material (LOT) series at the Äspö HRL in Sweden (Karnland et al, 2000), FEBEX experiment in Spain (Lloret & Villar, 2007), OPHELIE and PRACLAY heater experiments in Belgium (Li et al, 2006, 2010, Romero & Li, 2010) and Mock-Up-CZ experiment in Czech Republic (Pacovsky et al, 2007) etc. The experimental results and achievements obtained from these large-scale experiments provide important references on investigating the behaviors of bentonite under simulative nuclear radioactive waste repository conditions.

The performance of large-scale in situ tests is complicated and time-consuming and the boundary conditions in them are not always well controlled. For this reason, laboratory tests at different scales in which the conditions of the bentonite in an engineered barrier for HLW disposal are simulated are very useful to identify and quantify processes.

The work presented here started in the framework of the EC FEBEX project, for the study of the near field for a HLW repository in crystalline rock according to the Spanish concept (ENRESA, 2006). Among the laboratory tests started in the framework of the FEBEX Project-and continued in the NF-PRO Project-are those performed in cells in which the compacted bentonite is subjected simultaneously to heating and hydration, in opposite directions, in order to better understand the hydration process (Villar et al., 2005a, 2008). A series of infiltration tests performed under thermal gradient and dismantled after 0.5, 1, 2 and 8 years operation are presented in this paper and the results obtained concerning water intake and final water content and density of the bentonite are analyzed by means of a fully coupled THM formulation (Olivella et al., 1994).

The numerical analyses have been performed using the CODE_BRIGTH program (Olivella et al., 1996), which is a finite element code developed to handle coupled THM problems in porous media. The cells have been modeled as a boundary value problem. The geometry, initial conditions and boundary conditions have been adopted in order to reproduce as closely as possible the actual conditions of the tests. The modeling has considered the different stages of the tests, i.e. heating and hydration, cooling and dismantling (Villar et al., 2005b). The extensive experimental campaign carried out during the FEBEX project has allowed to determine and estimate the main parameters of the constitutive models related to the thermal, mechanical and hydraulic problems.

At the present stage, the Gaomiaozi (GMZ) bentonite is considered as the candidate buffer and backfill material for the Chinese repository. Lots of basic experimental studies have been conducted and favorable results have been achieved (Liu et al., 2003; Liu & Cai, 2007a; Ye et al. 2009a). In order to further study the behavior of the GMZ-Na-bentonite under relevant repository conditions, a mock-up facility, named China-Mock-up, was proposed based on a preliminary concept of HLW repository in China. The experiment is intended to evaluate THMC processes taking place in the compacted bentonite-buffer during the early phase of HLW disposal and to provide a reliable database for numerical modeling and further investigations.

In order to predict the long-term behavior of GMZ-Na-bentonite under physico-mechanical coupling condition, an essential objective of the China-Mock-up test consists to establish a numerical approach. In this regard, a constitutive model is proposed to tackle the

physical-mechanical behavior of GMZ-Na-bentonite. In the model, the following physical phenomena are taken into account: the transport of liquid (advection) and heat (convection and conduction), the vapor diffusion, the evaporation and condensation phenomena of water. The constitutive model of Alonso-Gens (1990) is used to reproduce the fundamental mechanical features of the GMZ bentonite in partially saturated condition. In order to validate the proposed model, a preliminary numerical simulation of the China-Mock-up test is carried out by the program LAGAMINE developed at Liege University (Charlier, 1987). The qualitative analysis of the predictive result is realized.

The overall approach is based on performing experiments according to the needs for additional studies on key processes during the early EBS evolution. The study will make use to the extent possible of on going experiments being conducted in the laboratory of Beijing Research Institute of Uranium Geology (BRIUG).

2. Theoretical formulation

i) CODE-BRIGHT

The THM formulation proposed by Olivella et al. (1994) has been adopted as a general framework for the analysis of the results of the thermo-hydraulic tests. The theoretical framework is composed of three main parts: balance equations, constitutive equations and equilibrium restrictions. The framework is formulated using a multi-phase, multispecies approach. The subscripts identify the phase ("*s*" for solid, "*l*" for liquid and "*g*" for gas), and the superscript indicates the species ("*h*" for mineral, "*w*" for water and "*a*" for air). The liquid phase may contain water and dissolved air, and the gas phase may be a mixture of dry air and water vapor. Dry air is considered as single species. Thermal equilibrium between phases is assumed. This means that the three phases are at the same temperature.

2.1 Balance equations

Equations for mass balance were established following the compositional approach, which consists of balancing the species rather than the phases. The mass balance of solid present in the medium is written as

$$\frac{\partial}{\partial t}(\rho_s(1-\phi)) + \nabla \cdot \left((\rho_s(1-\phi))u\right) = 0 \qquad (1)$$

Where ρ_S is the mass of solid per unit volume of solid, ϕ is the porosity, $\mathbf{j}_s$ is the flux of solid, t is time and ∇ is the divergence operator.

Water is present in liquid and gas phases. The total mass balance of water is expressed as

$$\frac{\partial}{\partial t}(\theta_l^w S_l \phi + \theta_g^w S_g \phi) + \nabla \cdot (j_l^w + j_g^w) = f^w \quad (2)$$

Where θ_l^w and θ_g^w are the masses of water per unit volume of liquid an gas respectively; S_l, is the volumetric fraction of pore volume, occupied by the alpha phase ($\alpha = l, g$); j_l^w and j_g^w denotes the total mass fluxes of water in the liquid and gas phases (water vapor) with respect to a fixed reference system and f^w is an external supply of water.

Dry air is present in liquid and gas phases. The total mass balance of dry air is expressed as

$$\frac{\partial}{\partial t}(\theta_l^a S_l \phi + \theta_g^a S_g \phi) + \nabla \cdot (j_l^a + j_g^a) = f^a \quad (3)$$

Where θ_l^a and θ_g^a are the masses of dry air per unit volume of liquid an gas, respectively; S_a is the volumetric fraction of pore volume, occupied by the alpha phase ($\alpha = l, g$); j_l^a and j_g^a denote the total mass fluxes of dry air in the liquid and gas phases with respect to a fixed reference system and f^a is an external supply of dry air.

Regarding the thermal problem, equilibrium between the phases is assumed. Therefore, the temperature is the same for all the phases. Consequently, only one equation is needed for the energy balance. The total internal energy, per unit volume of porous media, is obtained adding the internal energy of each phase corresponding to each medium. Applying the balance equation to this quantity, the following equation is obtained:

$$\frac{\partial}{\partial t}(E_s \rho_s (1-\phi) + E_l \rho_{lp} S_l \phi + E_g \rho_g S_g \phi) + \nabla \cdot (i_c + j_{ES} + j_{El} + j_{Eg}) = f^E \quad (4)$$

where E_s is the solid specific internal energy; E_l and E_g are specific internal energies corresponding to liquid and gas phase, respectively, ρ_S is the solid density; ρ_l and ρ_g are the liquid and gas phase densities; i_c is the conductive heat flux; $\mathbf{j}_{Es}$ is the advective energy flux of solid phase with respect to a fixed reference system; $\mathbf{j}_{El}$ and $\mathbf{j}_{Eg}$ are the advective energy flux of liquid and gas phases, respectively, with respect to a fixed reference system;

f^E are the energies supply per unit volume of medium.

Finally, the balance of momentum for the porous medium reduces to the equilibrium equation in total stresses:

$$\nabla \cdot \sigma + b = 0 \tag{5}$$

Where σ is stress tensors and *b* is the vector of body forces.

To solve in a coupled way the sets of equations presented above, one unknown (state variable) is associated to each balance equation (Eqs.(1)- (5)). Then, from the state variables, the dependent variables are calculated using the constitutive equations or the equilibrium restrictions.

2.2 Constitutive equations

The constitutive equations establish the link between the independent variables (or unknowns) and the dependent variables. In this section some constitutive laws will be introduced in a generic way, and the particular values of the parameters are given in Section 3. A more detailed explanation of the mathematical formulation in general and constitutive equations in particular is given in Gens et al. (1998). Concerning the hydraulic problem it is assumed that the liquid and gas flows follow Darcy's law:

$$\mathbf{q}_\alpha = -\mathbf{K}_\alpha (\nabla P_\alpha - \rho_\alpha g); \alpha = l, g \tag{6}$$

where P_l and P_g are liquid and gas pressure, respectively, $\mathbf{q}_l$ is the liquid density, $\mathbf{q}_g$ is the gas density, **g** is the gravity vector and **K**a is the permeability tensor of the alpha phase (*a* = *l*, *g*), which is given by

$$\mathbf{K}_\alpha = \mathbf{k} \frac{k_{r,\alpha}}{\mu_\alpha}; \alpha = l, g \tag{7}$$

The intrinsic permeability tensor (**k**) depends on the pore structure of the porous medium. k_{ra} is the value of relative permeability that controls the variation of permeability in the unsaturated regime and μ_α denotes the dynamic viscosity. α may stand for either *l* or *g* depending on whether liquid or gas flow is considered. The relative permeability of liquid (k_{rl}) phases is made dependent on S_e (effective degree of saturation) according to

$$k_{rl} = S_e^n \quad \text{(a)}; \qquad S_e = \frac{S_l - S_{lr}}{S_{ls} - S_{lr}} \quad \text{(b)} \tag{8}$$

Where S_l is degree of saturation, S_{lr} and S_{ls} are residual and maximum degree of saturation, respectively, and n is a material parameter. Another relevant law related to the hydraulic problem is the retention curve.

The molecular diffusion of vapor water in gas phase is governed by Fick's law, through

$$\mathbf{i}_g^w = -\mathrm{D}_g^w \nabla \omega_g^w = -(\phi \rho_g S_g \tau D_m^w \mathrm{I} + \rho_g \mathrm{D}'_g) \nabla \omega_g^w \quad (9)$$

Where $\mathbf{i}_g^w$ is the non-advective mass flux of water in gas, D_g^w is the dispersion tensor, ω_g^w is the mass fraction of water in gas, τ is the tortuosity and D'_g the mechanical dispersion tensor. D_m^w is the molecular diffusion coefficient of vapor in gas.

As for the thermal problem, the Fourier's law has been adopted for the conductive flux of heat. Thermal conductivity depends on the hydration state of the clay and is expressed by a variant of the geometric mean:

$$\mathbf{i}_c = -\lambda \nabla T \quad (10)$$

Where: $\lambda = \lambda_{sat}^{Se} \lambda_{dry}^{(1-s_e)}$ (11)

And $\lambda_{dry} = \lambda_{solid}^{(1-\phi)} \lambda_{gas}^{\phi}$; $\lambda_{sat} = \lambda_{solid}^{(1-\phi)} \lambda_{liq}^{\phi}$ (12)

Where, λ is the thermal conductivity.

Finally, regarding the mechanical problem, the constitutive model known as‘‘BBM" (Barcelona Basic Model) has been adopted. Due to the high compaction the bentonite blocks have been subjected to, the description of the behavior of the material inside the yield surface is particularly important. The variation of stress-stiffness with suction and, especially, the variation of swelling potential with stress and suction have been considered. The resulting elastic model is the following:

The mechanical law adopted is the Barcelona Basic Model (BBM). This model extends the concept of critical state for saturated soils to the unsaturated conditions, including the dependence of yield surface on suction. Two stress variables are considered: the net stresses and capillary suction. Net stress is the excess of total stress over gas pressure. If full saturation is achieved, net mean stress becomes effective stress. For simplicity net stress will also be denoted by σ.

A thermoplastic constitutive law (Alonso et al., 1990; Gens, 1995) has been selected based on a generalized yield surface that depends not only on stresses but on temperature and suction as well:

$$f = f(\sigma, \varepsilon_v^p, s, \Delta T) \tag{13}$$

$\Delta T = T - T_0$ is the temperature difference with respect to an arbitrary reference temperature, T_0. In terms of invariants:

$$F = f(p, J, \theta, \varepsilon_v^p, s, \Delta T) \tag{14}$$

Where,

$$P = (\frac{1}{3})(\sigma_x + \sigma_y + \sigma_z) \tag{15}$$

$$J^2 = 1/2\,\mathrm{trace}(s^2) \tag{16}$$

$$\theta = -\frac{1}{3}\sin^{-1}(1.5\sqrt{3}\det s / J^3) \tag{17}$$

$$s = \sigma - pI \tag{18}$$

I is the identity tensor. For simplicity, a form of the classical Modified Cam-clay model is taken as the reference isothermal saturated constitutive law:

$$F = \frac{3J^2}{g_y^2} - L_y^2(p + P_s)(P_0 - P) = 0 \tag{19}$$

Volumetric strain is defined as

$$\varepsilon_v = \varepsilon_x + \varepsilon_y + \varepsilon_z \tag{20}$$

And ε_v^p is the plastic volumetric strain.

The basic assumption is that the pre-consolidation pressure, P_o, is made dependent on both suction and temperature:

$$P_0 = P_c\left(\frac{P_c}{P^c}\right)^{\frac{\lambda(0)-k_{i0}}{\lambda(s)-k_{i0}}} \tag{21}$$

$$P_c = P_0^* + 2(\alpha_1 \Delta T + \alpha_2 \Delta T(T)) \tag{22}$$

$$L_y = \frac{M}{g_y(\theta = -\pi/6)} \tag{23}$$

$$\lambda_s = \lambda(0)[(1-r)\exp(-\beta s) + r \tag{24}$$

In addition

$$P_s = k\exp(-\rho\delta T)s \tag{25}$$

In common with other critical state models, it is assumed that hardening depends on plastic

volumetric strain only according to

$$\dot{P}_0^* = \frac{1+e}{\lambda(0)-k_{i0}} P_0^* \dot{\varepsilon}_v^p \tag{26}$$

And the plastic potential

$$G = \frac{3J^2}{g_p^2} - \alpha L_p^2 (p + P_s)(P_0 - p) \tag{27}$$

$$L_p = \frac{M}{g_p(\theta = -\pi/6)} \tag{28}$$

If α = 1, an associated plastic model results.

The variation of stress-stiffness with suction and, especially, the variation of swelling potential with stress and suction have been carefully considered. The resulting elastic model is as follows:

$$\dot{\varepsilon}_v^e = \frac{k_i}{1+e}\frac{\dot{P}}{P} + \frac{k_s}{1+e}\frac{\dot{s}}{s+0.1} + (\alpha_0 + 2\alpha_2 \Delta T)\dot{T} \tag{29}$$

$$k_i = k_{i0}(1 + \alpha_{is} S) \tag{30}$$

$$k_s = k_{s0}(1 + \alpha_{sp} \ln p / P_r) \exp(\alpha_{ss} s) \tag{31}$$

$$\dot{E} = \dot{J} / G; \quad G = E / 2(1+\nu) \tag{32}$$

Where *E* is the young module.

2.3 Equilibrium restrictions

Other types of relationships that relate dependent variables with unknowns are the equilibrium restrictions. They are obtained assuming chemical equilibrium for dissolution of the different species (dry gas and vapor) in phases (liquid, gas). This assumption is sufficiently adequate because these chemical processes are fast compared to the transport processes that take place in porous media and, for this reason; they are not rate-controlled. In this problem the concentration of water vapor in the gas phase is controlled by the psycrhometric law, and the solubility of dry gas in water is given by Henry's law.

ii) LAGAMINE

In order to reproduce the physical-mechanical behavior of the GMZ bentonite aforementioned, a coupled THM model is proposed. In the model, various THM coupling

phenomena are taken into account, including the transport of heat (conduction and convection), motion of liquid water, vapor diffusion, and their couplings with mechanical behaviors. The main formulations of the proposed model are presented in this part.

2.4 Constitutive model

2.4.1 diffusion model

In general, the compacted bentonite is composed of three phases, namely the solid, liquid water and gas (air and water vapor). In the simulations, the conservation mass of each phase (water or gas) is assumed. The phase exchange term thus will not be considered in the balance equations. The variables chosen for the description of the flow problem are liquid water pressure, gas pressure and temperature.

(1) water species

For the water species, the mass conservation equation is obtained by summing the balance equation of liquid water and water vapor. The equation includes the variation of water storage and the divergence of water flows in each phase. Considering water vapor is a component of gaseous phase, it thus has two contributions: the advective flux of gaseous phase and the non-advective flux of the water vapor related to vapor diffusion inside the gaseous phase, which can be written as (Collin et al., 1999):

$$\frac{\partial \rho_w n S_{r,w}}{\partial t} + \mathrm{div}(\rho_w \underline{f}_w) + \frac{\partial \rho_v n S_{r,g}}{\partial t} + \mathrm{div}(\underline{i}_v \rho_v \underline{f}_g) = 0 \tag{33}$$

where ρ_w is liquid water density; n is the medium porosity; $S_{r,w}$ is water saturation degree, $\underline{f}_\alpha$ (α=w,g) represents macroscopic velocity of the phase α; $\underline{i}_v$ is the non-advective flux of water vapour; ρ_v is water density; $S_{r,g}$ is the gas degree of saturation in volume and t is the time. The first two items in Eq. (33) are related to liquid water, and the latter two are associated with water vapour; ρ_v is water density; $S_{r,g}$ is the gas degree of saturation in volume and t is the time. The first two items in Eq. (33) are related to liquid water, and the latter two are associated with water vapour.

The generalized Darcy's law for multiphase porous medium is adopted to simulate the motion of liquid water:

$$\underline{f}_{\mathrm{w}} = -\frac{k_{\mathrm{int}} k_{\mathrm{r,\,w}}}{\mu_{\mathrm{w}}}[\underline{\nabla} p_{\mathrm{w}} + g\rho_{\mathrm{w}}\underline{\nabla} y] \tag{34}$$

where p_{w} is the liquid water pressure; y is the vertical upward directed co-ordinate; g is the gravity acceleration; μ_{w} is the dynamic viscosity of the liquid water, and k_{int} is the intrinsic permeability.

For the pores partially filled by air, it will be more difficult to constitute pathways for water flow, the permeability is consequently decreased. The variation of permeability with the saturation degree is taken into account by introducing the variable of water relative permeability $k_{\mathrm{r,\,w}}$.

The water vapor flow is assumed to follow Fick's diffusion law in a tortuous medium. In the study, the formulation proposed by the model of Philip and Vries (1957) is adopted:

$$\underline{i}_{\mathrm{v}} = -D_{\mathrm{atm}}\tau_{\mathrm{v}} n S_{\mathrm{r,g}}\underline{\nabla}\rho_{\mathrm{v}} \tag{35}$$

where D_{atm} is the molecular diffusion coefficient and τ_{v} is the tortuosity.

(2) Heat diffusion

In the context, one unique temperature variable is adopted. It means that the temperature is assumed to be homogenous in all phases. The heat transport is related to three effects: conduction, convection and vaporization, as presented in the following equation:

$$q' = -\Gamma\underline{\nabla} T + [c_{\mathrm{p,\,w}}\rho_{\mathrm{w}}\underline{f}_{\mathrm{w}} + c_{\mathrm{p,\,a}}(\underline{i}_{\mathrm{a}} + \rho_{\mathrm{a}}\underline{f}_{\mathrm{g}})] + c_{\mathrm{p,\,v}}(\underline{i}_{\mathrm{v}} + \rho_{\mathrm{v}}\underline{f}_{\mathrm{g}})(T - T_0) + (\underline{i}_{\mathrm{v}} + \rho_{\mathrm{v}}\underline{f}_{\mathrm{g}})L \tag{36}$$

where Γ is the medium conductivity; $c_{\mathrm{p,\,a}}$ (α=w, v, a) represents the specific heat of phase α. In general, the thermal conductivity is dependent on the temperature and saturation degree. For simplicity, the influence of temperature on thermal conductivity is not considered therein.

2.4.2 Mechanical model

The significant influence of saturation degree on the mechanical behavior of soil has been verified by numerous experimental studies, which should be taken into account in the mechanical modeling. Based on the experimental investigations, some constitutive models are proposed (Alonso, 1990; Alonso, 1999; Tang, 2009). The BBM model is widely used because of its capacity of representing the main fundamental features of partially saturated soils in a consistent and unified manner. It should be noted that the expensive behavior of compacted bentonite is better represented with the modified BBM model (Alonso et al., 1999)

by taking into account of the microstructural variation during wetting process. However, the formulation of the model is much more complicated, and some parameters are difficult to identify. As a preliminary study, the BBM model is adopted. A brief introduction to this model is given.

(1) Yield surface

The BBM model is based on the classic Cam-clay model. In consideration of the influence of saturation degree on the mechanical behavior, suction is adopted as an independent variable in this model. The plastic yield surface is thus written in three-dimensional stress space (*p*, *q*, *s*). For the BBM model, the yield surfaces are composed of three parts. In the (*p*, *q*) space, for a given suction, the yield surface can be written as:

$$q^2 - M^2(p + p_s)(p_0 - p) = 0 \tag{37}$$

where p is the mean stress; q refers to the deviatoric stress; M is the slope of the critical line, and p_s represents the soil strength in extension.

The pre-consolidation pressure p_0 varies with the suction. The following equation is proposed which is well known as the LC curve:

$$p_0 = p_c \left(\frac{P_0^*}{p_c} \right)^{\frac{\lambda(0)-k}{\lambda(s)-k}} \tag{38}$$

where P_0^* is the pre-consolidation pressure in saturated condition; p_c is a reference pressure; k is the elastic slope of the compressibility curve against the net mean stress; $\lambda(0)$ is the plastic slope for the saturated condition, and $\lambda(s)$ refers to the plastic slope of the compressibility curve against the net mean stress (Fig. 1).

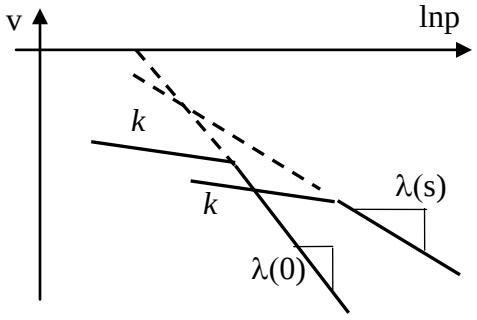

Fig. 1 Compression curve for saturated and unsaturated soil.

Under unsaturated condition, the suction contributes to stiffening the soil against the

external load. Hence, the plastic slope of the compressibility curve varies with the suction. The following equation is proposed to represent this phenomenon:

$$\lambda(s) = \lambda(0)[(1-r)\exp(-\beta s) + r] \tag{39}$$

where γ and β are the parameters describing the changes in soil stiffness with suction. The LC curve defines another part of the yield surface used for modeling the collapse behavior under wetting.

Numerous studies confirmed that irreversible volumetric deformation may be induced by variations in suction. Therefore, the SI yield surface, which defines the maximum previously attained value of the suction, is employed to take into account this phenomenon:

$$F_2 = s - s_0 = 0 \tag{40}$$

where s_0 represents the maximum historic suction submitted to the soil.

(2) Hardening law

The evolution of yield surfaces is assumed to be controlled by the total plastic volumetric strain ε_v^p. Two hardening laws define the evolution of state variables p_0 and s_0 with the irreversible strain:

$$\mathrm{d}p_0^* = \frac{(1+e)p_0^*}{\lambda(0)-\kappa}\mathrm{d}\varepsilon_v^p \tag{41}$$

$$\mathrm{d}s_0 = \frac{(1+e)(s_0+P_{at})}{\lambda_s - k_s}\mathrm{d}\varepsilon_v^p \tag{42}$$

Where e is the porosity of the soil; P_{at} is the atmospheric pressure; λ_s and k_s are the plastic and elastic stiffness parameters for suction variation, respectively.

3. Material and THM parameters

3.1 FEBEX bentonite

The bentonite is extracted from the Cortijo de Archidona deposit (Almeria, Spain). Processing of the material at the factory consisted in disaggregation and gently grinding, drying at 60℃ and sieving by 5 mm. For the large-scale tests of the Project, the bentonite blocks were manufactured by uniaxial compaction of the granulated clay with its hygroscopic water content, at dry densities close to 1.7 g/cm^3 (ENRESA, 2006).

The FEBEX bentonite has a content of montmorillonite higher than 90% with variable

quantities of quartz, plagioclase, K-feldspar, calcite and opal-CT (cristobalite-trydimite). The cation exchange capacity (CEC) varies from 96 to 102 meq/100 g. Major exchangeable cations are: Ca (35-42 meq/100 g), Mg (31-32 meq/100 g), Na (24-27 meq/100 g) and K (2-3 meq/100 g).

The liquid limit of the bentonite is 102±4%, the plastic limit is 53±3%, the specific gravity 2.70±0.04, and 67±3% of particles are smaller than 2 μm. The hygroscopic water content in equilibrium with the laboratory atmosphere is 13.7±1.3%. The external specific surface area, using the BET technique, is 32±3 m^2/g and the total specific surface area, using the hygroscopicity method, is about 725 m^2/g. The analysis of the mercury intrusion data reveals that the intra-aggregate pores (smaller than 0.006 μm) represents the 73-78% of total pore volume when the bentonite is compacted at a dry density of 1.7 g/cm^3.

3.2 THM parameter of FEBEX bentonite

The saturated permeability to deionised water, **k** (Eq. (7)), of samples of untreated FEBEX bentonite compacted at different dry densities can be related with porosity through a modified Kozeny's law according to

$$\mathbf{k} = k_0 \frac{\phi^3}{(1-\phi)^2} \frac{(1-\phi_0)^2}{\phi_0^3} \mathbf{I} \tag{43}$$

where k_0 is the intrinsic permeability corresponding to ϕ_0 (a reference porosity).

The retention curve of the bentonite was determined in samples compacted to different dry densities (Lloret et al., 2004). The volume of the samples remained constant during the determinations, since they were confined in constant volume cells. To impose the different relative humidities the cells were placed in desiccators with sulphuric acid solutions of various concentrations. A modified van Genuchten law has been adopted to model the dependence of the degree of saturation on suction

$$S_e = \left[1 + \left(\frac{s}{P_0}\right)^{\frac{1}{1-\lambda_0}}\right]^{-\lambda_0} f_d; \qquad \text{where: } f_d = \left(1 - \frac{s}{P_d}\right)^{\lambda_d} \tag{44}$$

where s ($s = P_g - P_l$), is the suction, P_0 is a parameter related to the capillary pressure (the air entry value) and k_0 is a parameter that controls the shape of the curve (van Genuchten, 1978).

The function f_d is included to obtain more suitable values at high suctions, P_d is a parameter related with the suction at 0 degree of saturation and k_d is a model parameter (when it is null, the original model is recovered). The adopted parameters are: P_0 = 28 MPa, k_0 = 0.18, P_d = 1100 MPa, λ_d = 1.1 and η= 0.7.

The relation between P_0 and surface tension (σ) suggested by Olivella and Gens (2000) has been extended to this model, that is

$$P_0 = P_{T_0}\frac{\sigma_T}{\sigma_{T_0}} \tag{45}$$

where the surface tension (in N/m) has been obtained fitting values of surface tension with the following expression (Olivella, 1995):

$$\sigma_T = 0.03059\exp\left(\frac{252.93}{273.15+T}\right) \tag{46}$$

By varying P_0 in accordance with this expression, a dependence of the retention curve with temperature is introduced. Therefore, suction will decrease with temperature for a given degree of saturation (Olivella and Gens, 2000). Experimental results have shown that, in most cases, the influence of temperature on retention curve is small (Lloret et al., 2004).

The thermal conductivity, λ (Eq. (10)) of the compacted bentonite at laboratory temperature is related to the degree of saturation S_e (Eq. (11)). A value of 0.47 has been adopted for λ_{dry} and 1.15 for λ_{sat}.

Some isothermal infiltration tests and heat flow tests at constant overall water content were performed during FEBEX I and they were back-analyzed using CODEBRIGHT (Pintado et al., 2002). It is possible to fit the experimental data for the relative permeability law (Eq. (8)) assuming a cubic law (i.e. n = 3). As for the tortuosity factor, τ (Eq. (9)), a value of 0.8 has been proposed.

Regarding the mechanical properties, the THM version of the BBM presented in section 2 has been adopted in this analysis. However, the BBM being not able to reproduce the swelling behavior of the bentonite, a number of modifications have been introduced in the elastic part of the model in order to reproduce the expansive behavior of the FEBEX bentonite. Due to the high pressures applied to compact the bentonite blocks, the description of the behavior of the material inside the yield surface is particularly important. The variation of stress-stiffness with suction and, especially, the variation of swelling potential with stress

and suction have been considered. The resulting elastic model was introduced above (Eqs. (29) - (32)).

The parameters of the mechanical model were adopted during the pre-operational stage of the FEBEX project (ENRESA, 2006). The main model parameters are summarized in Table 1.More details can be found in Sanchez and Gens (2006).

Table1 Model parameters related to the mechanical problem (defining the Barcelona Basic Model).

κ	0.04	κ_s	0.25
ν	0.4	α_{is}	-0.003
α_{sp}	-0.147	α_{ss}	0.00
α_o	1.5×10^{-4} ($^oC^{-1}$)	α_2	0.00
λ_0	0.15	p_c	0.10 MPa
p_o^*	14 MPa	α	0.395
r	0.75	β	0.05
M	1.5	T_o	20 °C
k	0.1	ρ	0.2

3.3 GMZ bentonite

The GMZ bentonite is extracted from the northern Chinese Inner Mongolia autonomous region, 300 km northwest from Beijing. In this region area, around 120 million tons of Na-Bentonite reserves have been identified, and the mine area is about 72 km^2. The deposit is formed in later Jurassic period (Liu et al., 2007a). Based on the fundamental studies carried out, the GMZ bentonite is found to have ideal thermal, hydraulic, mechanical and physico-chemical properties of buffer material (Ye et al., 2009a). In this part, the main THM properties are summarized.

According to the X-diffraction analysis, the clay mineralogy is dominated by Montmorillonite (75.4%) which is essential mineral to ensure the sealing properties. Besides, the GMZ contains variable quantities of quartz (11.7%), cristobalite (7.3%), feldspar (4.3%) and kaolinite (0.8%) (Ye et al., 2009a). The relatively high content of montmorillonite results in a high Cations Exchange Capacity (CEC=77.30 meq/100g), a large plasticity index

(I_p=275), and large specific surface area (S=570m^2/g) (Cui et al., 2011). The major exchangeable cations are Na^+(43.56meq/100g), Ca^{2+}(29.14meq/100g) and Mg^{2+}(12.33meq/100g). Therefore, GMZ bentonite can be classified as Na-Bentonite.

The thermal conductivity of GMZ bentonite is found to increase as the dry density and water content increase (Liu et al., 2007a, 2007b). Concerning the hydraulic properties, the water retention curve at room temperature under confined and unconfined conditions is obtained by Chen et al. (2006). The influence of temperature on the soil-water characteristics of highly-compacted GMZ bentonite is also studied (Ye et al., 2009b). It is revealed that the water retention capacity of the highly-compacted GMZ bentonite decreases as the temperature increases.

The mechanical behaviors of GMZ bentonite are also investigated. A swelling pressure about 4.3MPa is measured for the GMZ bentonite with dry density of 1750Kg/m^3, and a relationship is established between the swelling pressure and the initial dry density (Ye et al, 2007). The mechanical loading test at controlled suction and temperature is carried out by Cui et al. (2011), and an elasto-plastic mechanical behavior with a clear change in slope is observed.

3.4 THM parameter of GMZ bentonite

(1) Hydro-thermal properties

Among the hydro-thermal properties, the water retention curve and permeability are considered as the key factors on the water intake volume and the final saturation degree. Measured data of water content in function of suction is available (Chen et al., 2006). The relation between suction and water saturation is adopted in the study:

$$S_{r,w} = S_{r,res} + a_3 \frac{S_{r,u} - S_{r,res}}{a_3 + (a_1 s)^{a_2}} \tag{11}$$

where $S_{r,u}$ is the maximum saturation degree in the soil and $S_{r,res}$ is the residual saturation degree for a very high value of suction.

Values of $S_{r,u}$ and $S_{r,res}$ determined in test are 1.0 and 0.1, respectively. Calibration of this function on measured data gives the values of the following parameters: a_1=3.5×10^{-6} Pa^{-1}, a_2=0.8, a_3=90. Water retention curve of GMZ bentonite is illustrated in Fig. 1.

Relative permeability curves are determined based on the experimental investigation (Ye et

al., 2009b), as shown in Fig. 2. The intrinsic permeability k_{int}= 2.0×10^{-21} m^2 is chosen according to the experimental data. Thus, we have

$$k_{r,w} = \frac{(S_{r,w} - S_{r,res})^4}{(S_{r,u} - S_{r,res})^4} \tag{12}$$

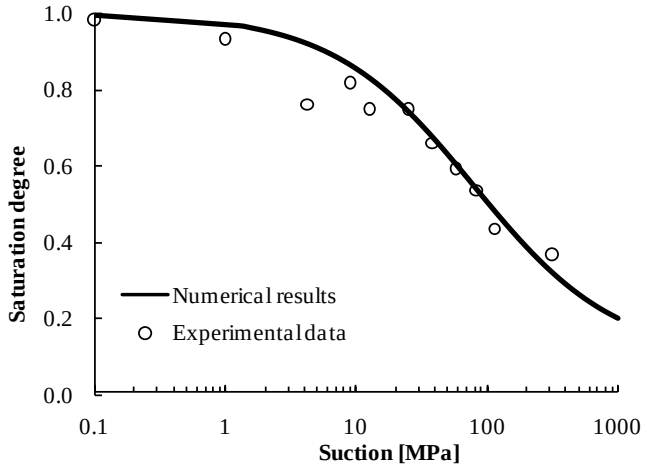

Fig. 1 Water retention curve of GMZ bentonite.

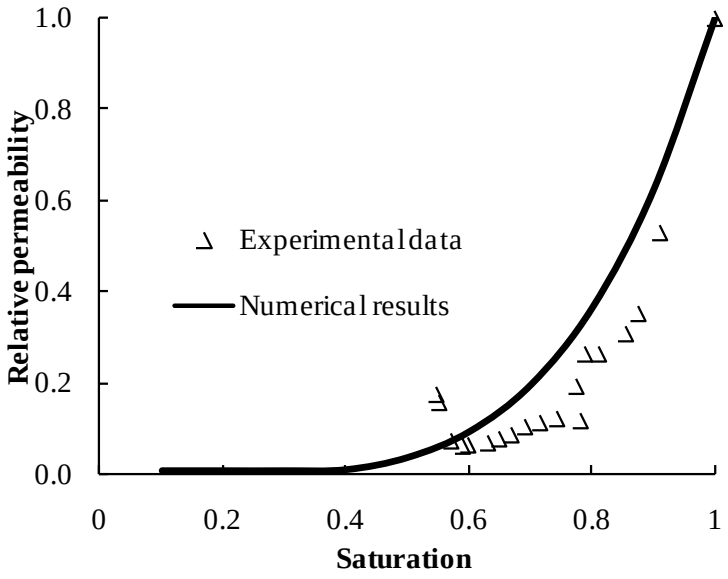

Fig. 2 Variation of relative permeability in function of saturation degree.

A linear relation is adopted to describe the variation in thermal conductivity with saturation

degree, as shown in Fig. 3. Table 1 summarized the other parameters of the hydraulic and thermal properties:

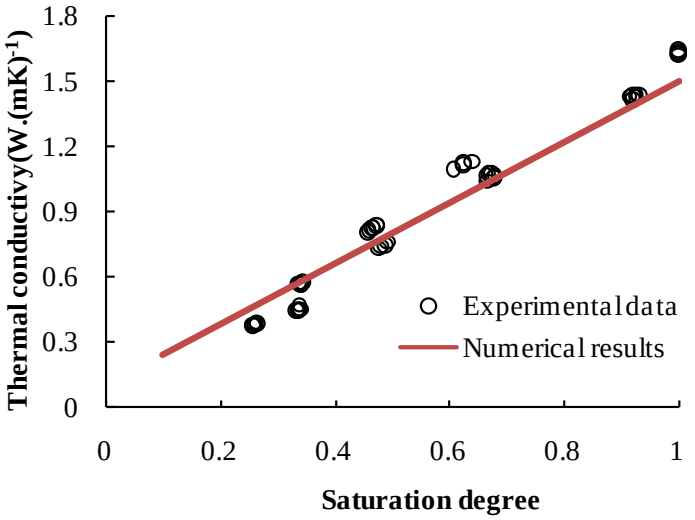

Fig. 3 Variation of thermal conductivity with saturation degree.

Table 1 Parameters of the flow model.

Grain density ρ_s (kg.m^{-3})	Grain specific heat $c_{p,s}$ (J.kg^{-1}K^{-1})	Water density ρ_w(kg.m^{-3})	Water dynamic viscosity μ_w(Pa.s)	Water specific heat $c_{p,w}$ (J.kg^{-1}K^{-1})	Air density ρ_a (kg.m^{-3})
1.6×10^{3}	2.6	1.0×10^{3}	1.009×10^{-3}	4.18×10^{3}	1.205
Air dynamic viscosity μ_a(Pa.s)	Air specific heat $c_{p,a}$ (J.kg^{-1}K^{-1})	Water vapour specific heat $c_{p,v}$ (J.kg^{-1}K^{-1})	Latent heat of vaporization L(J.kg^{-1})	Tortuosity, τ	
1.80×10^{-5}	1.0×10^{3}	1.90×10^{3}	2.50×10^{6}	0.1	

(2) Mechanical parameters

The mechanical loading test at constant suction and temperature (Cui et al. 2011) revealed that elastic stiffness parameters k and plastic stiffness parameters λ(s) of the GMZ bentonite increase with decrease of suction but are independent of the temperature changes. The effect of temperature on the yield stress p_0 of the GMZ bentonite is found to be insignificant. For simplicity, a constant value of the elastic stiffness parameter k is adopted. The parameters γ and β which define the variation of $\lambda(s)$ with suction, are determined based on experimental data (Fig. 4).

The LC curve describes the evolution of p_0 with suction, which depends on k, λ(s) and p_c. The reference pressure p_c cannot be directly determined, thus a calibration procedure is adopted. The stiffness parameters k_s and λ_s define the volumetric strain changes induced by suction. According to the experimental study, a volumetric strain of 32.4% is obtained when the suction is decreased from 110 to 9 MPa. Considering that the volumetric strain is induced in a wetting procedure (inferior to the maximum historic suction), it can be considered as elastic volumetric strain. Therefore, a value of 0.07 is determined for k_s. Due to the lack of experimental data, an average value of λ_s obtained from other types of Bentonite (0.25) is taken in the simulation (Collin et al., 1999). Based on the water retention curve, s_0 can be fixed from the initial saturation degree.

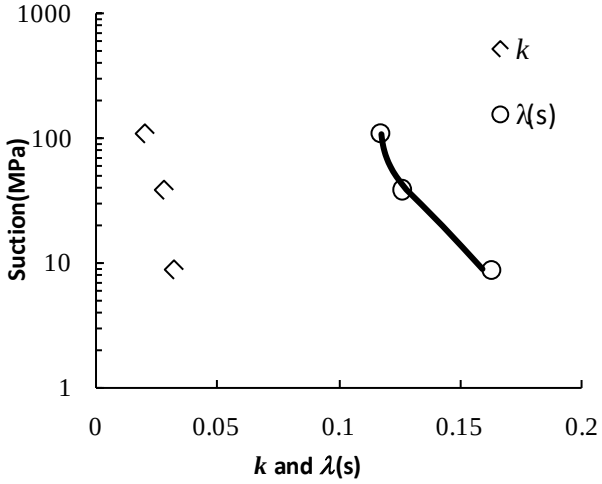

Fig. 4 Variation of k and λ(s) with suction.

The dependence of these parameters on the stress state generated in the soil sample is not taken into account. The values of parameters used in the simulations are summarized in Table 2.

Table 2 Parameters employed in mechanical model.

Saturated virgin compression index $\lambda(0)$	Elastic compression index k	Saturated pre-consolidation pressure p^*_0 (MPa)	Elastic stiffness index upon suction k_s	Plastic stiffness index upon suction λ_s	Maximum value of the suction s_0 (MPa)
0.18	0.027	0.6	0.08	0.25	80
Reference stress p_c (MPa)	Ratio $\lambda(s)/\lambda(0)$ for high suction γ	Parameters to control the increase of stiffness with suction β (MPa^{-1})			
0.45	0.65	0.045			

4. Experiment

i) FEBEX

A series of infiltration tests in large-scale cells (inner length 60 cm, internal diameter 7 cm) was running for different periods of time (0.5 to 7.6 years). The cells were made of Teflon to prevent lateral heat conduction, and externally covered with steel semi-cylindrical pieces to avoid deformation of the cell by bentonite swelling. Six 10 cm height blocks of FEBEX clay compacted with its hygroscopic water content at an initial nominal dry density of 1.65 g/cm^3, were piled up inside each cell. The actual average initial water content of the bentonite in the seven tests performed was 13.6%, and the average initial dry density was 1.66 g/cm^3.

The bottom part of the cell was a flat stainless steel heater set during the tests at a temperature of 100^{o}C, which is the temperature expected on the surface of the waste container in the Spanish concept. Over the upper lid of the cell there was a deposit in which water circulated at room temperature (20-30^{o}C).

Hydration with granitic water (salinity 0.02%) took place through the upper surface under an injection pressure of 1.2 MPa. The water intake was measured as a function of time in some of the tests with electronic equipment placed at the entrance of the cell (LVDT displacement transducer that allows measuring changes of volume with an accuracy of 0.001 cm^3).

In addition, the cells were instrumented with thermocouples inserted in the bentonite at different levels along the column. The number of thermocouples in each cell was 2, 3 or 5. Only the 7.6-year duration test was not instrumented with thermocouples (Fig. 5).

Seven tests were performed: two of 0.5 year duration, two of 1 year duration, two of 2 years duration and one of 7.6 years duration. Of the duplicate tests, the FQ ones were used for postmortem determination of hydro-mechanical properties, and the HI ones for postmortem determination of geochemistry and extraction of interstitial water. The longest test, CG3, was used for both kinds of postmortem determinations.

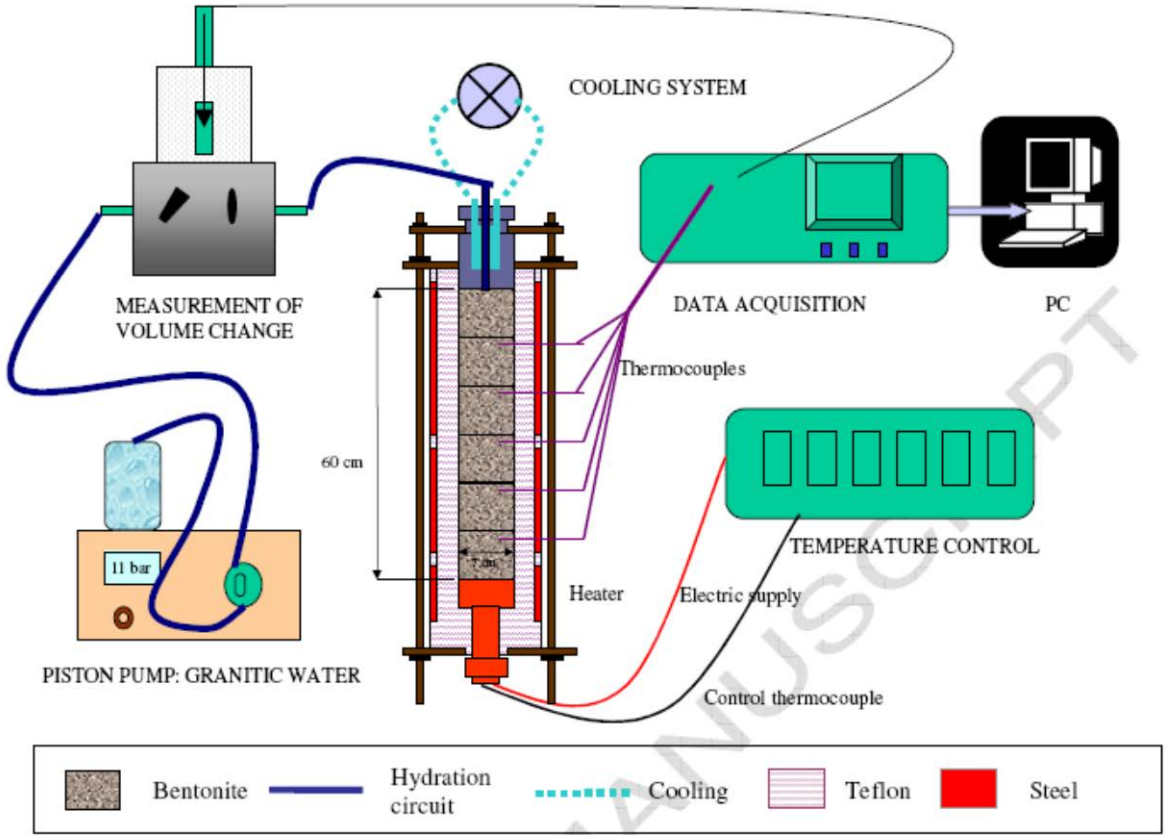

Fig. 5 Experimental setup for the infiltration tests.

At the end of the thermo-hydraulic treatment, the cells were dismantled and the clay blocks extracted. Special care was taken to avoid any disturbance in the conditions of the clay, particularly its dry density and water content. Once extracted, the bentonite columns were sawed in 24 cylindrical sections of 2.5 cm in thickness (numbered from 1, near the hydration surface, to 24, close to the heater). In the case of FQ tests, they were used for the following determinations: dry density, water content, swelling capacity, swelling pressure, permeability, porosity. In the case of HI tests, the samples were used for the determination of: dry density, water content, geochemistry (soluble salts, exchangeable cations, extraction of interstitial water) and scanning microscopy analysis. The samples from test CG3 were used for determination of dry density, water content, swelling capacity, specific surface area, mineralogy and geochemistry. This paper analyses only the results on final dry density and water content.

The gravimetric water content (w) was determined by oven drying at 110^{o}C for 24 hours

(defined as the ratio between the weight of water and the weight of dry solid). Dry density (ρ_d) is defined as the ratio between the weight of the dry sample and the volume occupied by it prior to drying. The volume of the specimens was determined by immersing them in a recipient containing mercury and by weighing the mercury displaced, as established in UNE Standard 7045 ‘‘Determination of soil porosity”.

ii) China-mock-up

The China-Mock-up is mainly made up of eight components, namely compacted bentonite blocks, steel tank, heater and corresponding temperature control system, hydration system, sensors, gas measurement and collection system, real-time data acquisition and monitoring system (Fig. 6).

It is assumed that the duration of the China-Mock-up experiment will not be shorter than 4 years. Then, after a cooling period, the experiment will be dismantled and all the available results will be collected and evaluated.

The China-Mock-up experiment was assembled completely on 10th September 2010. The real-time data acquisition and monitoring system has recorded all the measurement data from1st April 2011. And the heater was switched on to reach a low temperature at 30°C from 1st April 2011 until 8th July 2011. The T-H-M-C experiment was commenced on 8th July 2011, then the power rises at 1°C/d to reach a maximum temperature at 90°C, and the hydration system inject at 0.5MPa with Beishan groundwater at the working time, and the injection rate is 400g/d, and later raises to 600g/d.

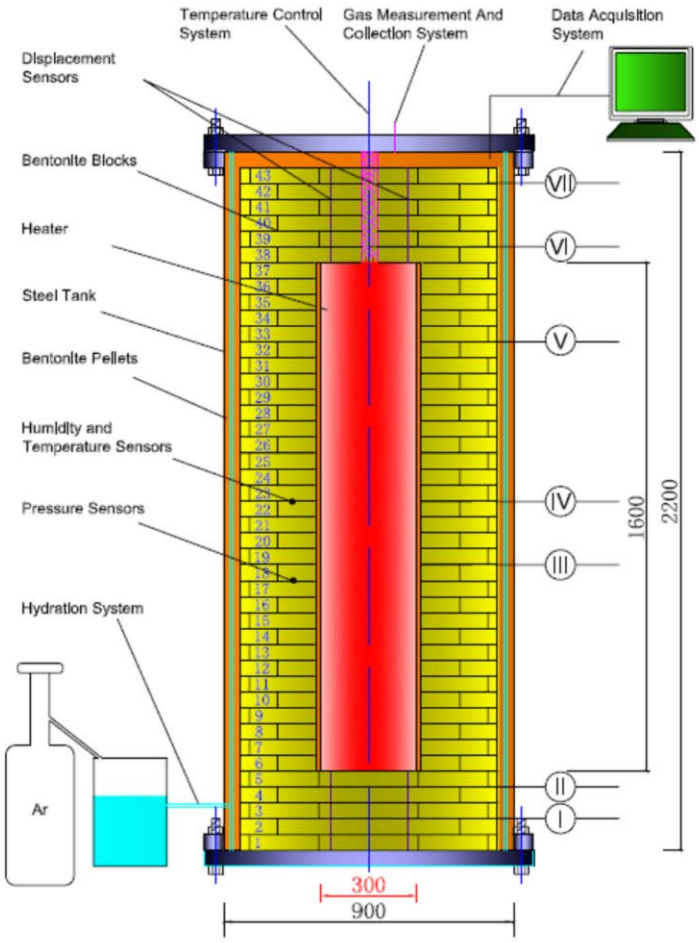

Fig. 6 Sketch of the China-Mock-up facility (unit: mm).

5. Numerical simulations

5.1 Boundary Conditions

i) CODE_BRIGHT

The finite element program CODE_BRIGHT (Olivella et al., 1996) has been used to analyze the cells as a boundary value problem. 1D axis-symmetrical models have been used in these analyses. A mesh of one hundred (100) elements has been chosen. A sensitivity analysis has also been carried out to verify that the model results do not depend on the mesh. The initial and boundary conditions of the model have been imposed in order to be the closest possible to the experiments. The initial water content of the bentonite block is close to

14%, from the retention curve adopted an initial value of suction close to 140 MPa has been chosen. An initially uniform temperature of 22^{o}C is assumed. Initial hydrostatic stresses of 0.15 MPa have been adopted. Regarding the boundary conditions a temperature of 100^{o}C is imposed at the contact between heater and bentonite (the bottom of the cell), while a constant water pressure of 1.2 MPa is imposed at the other extreme of the cell (upper part). The thermal boundary condition along the sample has been adopted in order to adjust the temperature field, in that sense a temperature of 23^{o}C has been fixed with a radiation coefficient of 1 (one). Regarding the mechanical problem, a small expansion of the cell has been allowed, in order to account for the deformability of the Teflon walls upon saturation and swelling of the bentonite that caused and overall decrease of its dry density, as it will be shown in this paper. Finally, a constant gas pressure (0.1 MPa) has been adopted in the analyses.

ii) LAGAMINE

In order to validate the proposed, the numerical simulation of the China-Mock-up test is carried out in this part. A 2D-axisymetric finite element simulation is realized with the help of the software LAGAMINE. The geometry and boundary conditions are illustrated in Fig. 7.

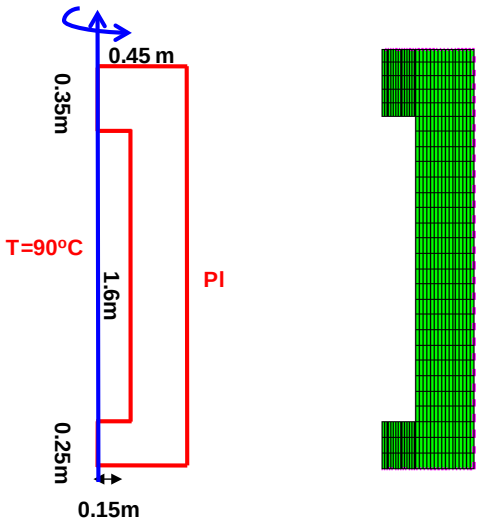

Fig. 7 Boundary conditions and mesh.

For simplicity, the steel tank is neglected to address the problem in the numerical test. The fixed horizontal/vertical displacement is imposed on the nodes in contact with the steel and

the heating is simulated by imposing the temperature on the nodes in contact with the heater. The hydration influence is modeled by increasing water pressure on the nodes of outer boundary. The convection transfer between the GMZ bentonite and atmosphere is simulated thanks to frontier thermal elements. In the simulations, air flow is not considered, whereas the vapor diffusion is assumed.

The system is initially at temperature of 20 °C. The gas pressure is assumed to be constant in order to have a better numerical convergence. The compacted GMZ bentonite has an initial water saturation of 48% and a void ratio of 0.57. According to the water retention curve determined, a suction of 80MPa is initially employed. As aforementioned, the dissolved air will not be taken into account.

Following the experimental procedure, the numerical simulation is divided into two phases: firstly, the temperature on the boundary connected to the heater and the water pressure on the outer boundary are increased respectively to 90 °C and 2MPa in 10 hours. In the following, the boundary conditions applied previously are kept constant in 3 years.

5.2 Experimental and numerical results

i) CODE_BRIGHT

The initiation of the thermo-hydraulic tests followed this procedure: first the temperature of the upper cooling circuit was set to 30^{o}C, after 24-48 h the temperature of the bottom heater was set to 100^{o}C and hydration started almost simultaneously (except in tests FQ1/2, HI1/2 and FQ2, in which hydration started 24 h afterwards). During the hydration-heating tests temperature measurements in different positions along the columns and water intake measurements (only in four of the tests) were performed.

During the TH tests, temperature was measured at different positions along the columns. In test CG3 no thermocouples were inserted. The temperatures quickly stabilized (in less than 200 h) and afterwards, they were mainly affected by the room temperature, reflecting the daily and seasonal changes, especially in the zones farther from the heater (Fig. 8). The average temperatures recorded by each thermocouple for the period between 700 h after the beginning of the tests and the end of the tests are plotted in Fig. 9. There are is a good agreement between the average temperatures measured in the duplicate tests of the same duration. There is a sharp temperature gradient in the vicinity of the heater, decreasing from

100°C at the heater surface to 50°C, 10 cm inside the clay. In addition, a decrease of temperature with saturation (longest tests) is observed, especially in the wettest zones, i.e. within the closest 40 cm to the hydration surface. This is due to the higher heat dissipation of the wet clay.

Since the model only intends to capture the whole thermal evolution of the test, the cyclic variations of temperature (due to the changes in the laboratory temperature) are not taken into account. Considering that, it can be seen that the model captures quite well the thermal field prevailing in the cell (Figs. 8 and 9).

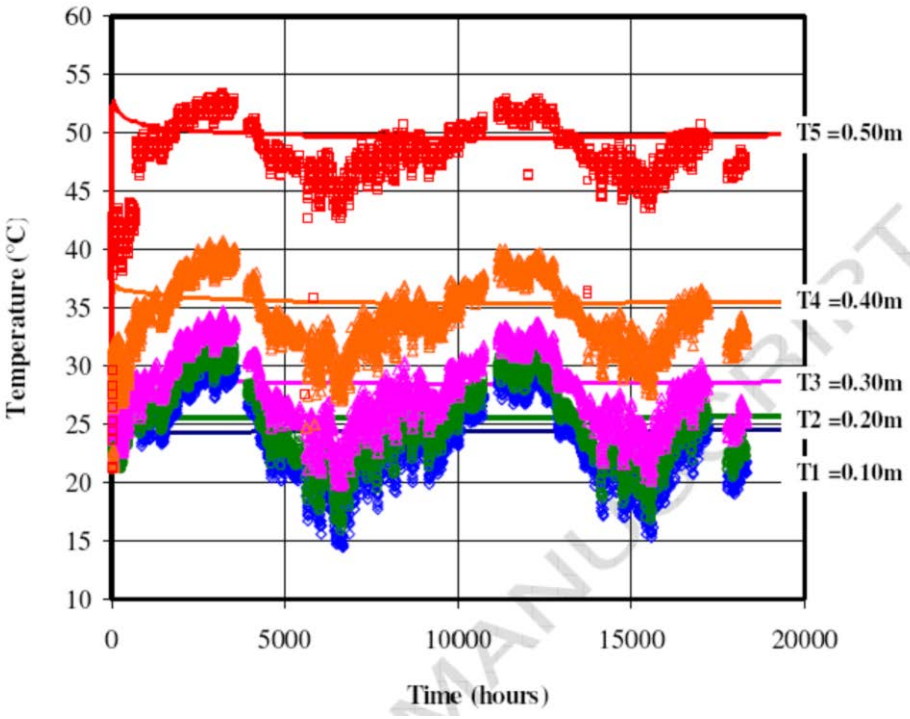

Fig. 8 Temperatures recorded by thermocouples in test HI2 (T1 to T5 were placed at 50, 40, 30, 20 and 10 cm from the heater, respectively): experimental and modeling results.

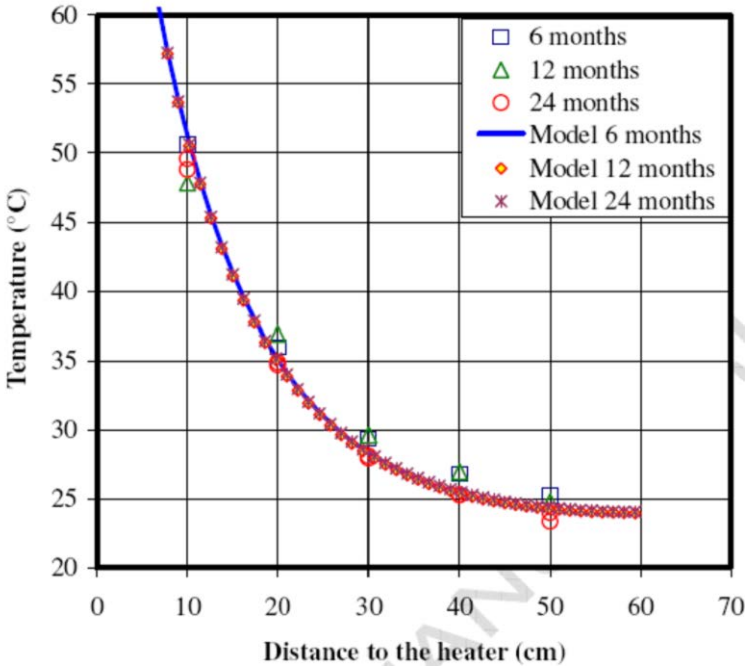

Fig. 9 Average steady temperatures at three different positions inside the clay for tests of different duration: experimental and modeling results.

The longest test, test CG3, had no thermocouples inserted in the clay, but before switching off the heater, the temperatures on the Teflon surface of the cell were measured with a hand-held thermistor thermometer. Although the external temperatures were lower than those inside the bentonite, a higher thermal gradient was observed in the proximity of the heater, and a soft decrease in the farthest area, where the temperature was very close to the room temperature at the moment of dismantling (22^{o}C).

Immediately after setting the heater temperature or after 24 h, depending on the particular test, hydration started. In some of the tests (FQ1/2, HI1/2, FQ2 and CG3) the water intake was also measured online. The water intake curves (Fig. 10), as measured by the volume change apparatuses, show disparity at the beginning of the tests, but tend to coincide as hydration progresses. The initial discrepancy is particularly clear for the two shortest tests, and can be mostly attributed to the different room temperature during the operation of both tests: test FQ1/2 operated in spring/summer and test HI1/2 in autumn/winter, for which reason the water intake was higher in the first test, since temperature increases permeability. It can be observed that the numerical results related to the hydraulic problem are quite good;

the cumulative water intake is well captured by the model.

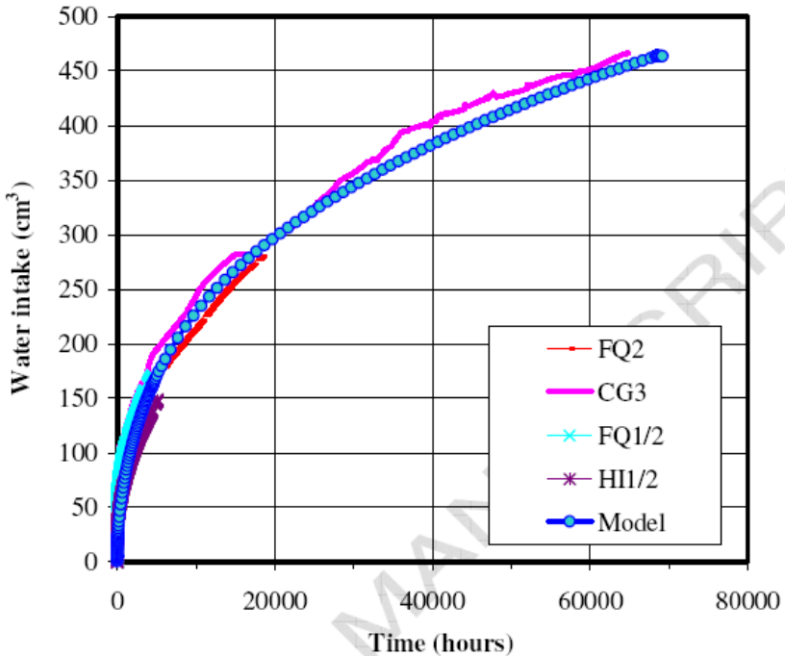

Fig. 10 Water intake during different duration tests: experimental and modeling results.

After switching off the heater and stopping the water injection, the cells were disassembled and the column of bentonite was extracted and weighed. In the longest test, CG3, the six bentonite blocks were sealed among them, although upon desiccation the two lower blocks could be detached. However, in the 1- and 2-year tests only the two upper blocks were sealed, i.e. the joint placed at 10 cm from the hydration surface, and in the 0.5-year tests no joint was sealed. Shrinkage cracks near the heater were not observed in any of the tests.

The swelling of the hydrated bentonite might have deformed the Teflon walls of the cell, what would be confirmed by the higher difficulty of extracting from the cells the upper, most hydrated blocks. In fact, the diameter of the bentonite column at the end of test CG3 was not constant along it, and it overall had increased with respect to the initial diameter of 7.03 cm. The inner diameter of the Teflon cell measured after disassembling and cooling ranged from 7.28 cm near the hydration surface to 7.05 cm near the heater, with an average value of 7.18 cm. This increase is due to the deformation of the Teflon walls caused by the swelling of the bentonite upon saturation, which also implied an overall decrease of the dry density of the bentonite during the test to a value of 1.57 g/cm^3, according to these diameter measurements.

Since the saturation of the bentonite in the shortest test was lower, it is expected that its overall swelling, and consequently its deformation and density decrease, was less important.

After slicing the columns, water content and dry density of each section were determined in two or three subsamples for most of the sections, although in some cases only one determination per section could be done. The distribution of water content along the bentonite column in the TH tests (Fig. 11), where an important gradient can be observed even in the longest test, shows the water content increased within the closest 20 cm from the hydration surface in the 6-month test, and within 40 cm in the 12- and 24- month tests. In the 7.6-year test the increase of water content took place all over the column except in the 10 cm closest to the heater. The water content reduction by the temperature effect is similar for the three shorter durations, which means that desiccation takes place rather quickly and only affects the closest 18 cm to the heater, where the water contents are lower than the initial ones, which were around 14%. After 6 months, the closest 18 cm to the heater experienced a desiccation that is not recovered after 24 months; hence the water content remained in this zone below the initial value, being close to 6% in the vicinity of the heater. After 7.6 years of testing the water content of the bentonite is lower than the initial one only in the 5 cm closest to the heater.

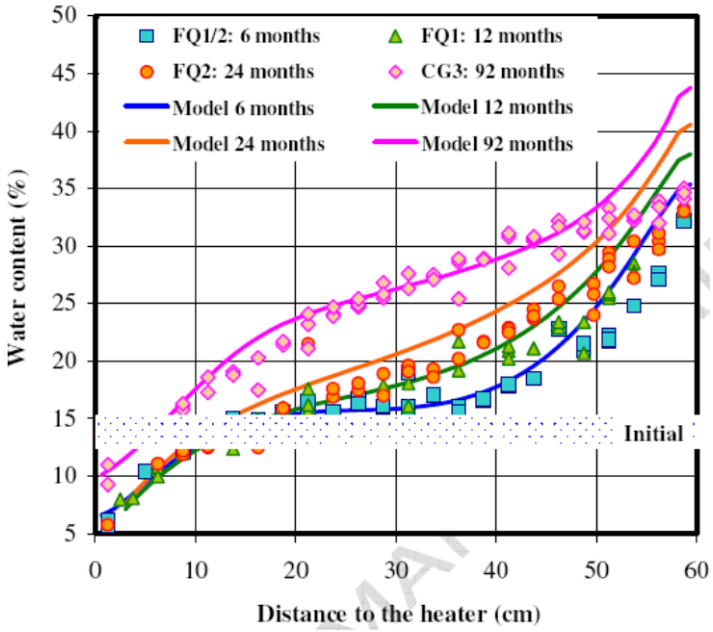

Fig. 11 Final water contents along the bentonite columns of the different tests: experimental and modeling results.

The dry densities gradient along the bentonite column at the end of the tests (Fig. 12) reflects the different swelling of the bentonite, since the more hydrated sections have swollen more. The dry density decreases from the heater towards the hydration surface following an approximately linear trend. In the zones affected by hydration, the densities decreased below the initial value (nominal 1.65 g/cm^3) due to the expansion caused by saturation. On the contrary, near the heater, the dry density increased, due to the shrinkage caused by desiccation. Despite the dispersion of the data-caused by the initial inhomogeneities and by the determination method, it can be observed that the densities reached near the hydration surface were lower as the duration of the test increased (values as low as 1.41 g/cm^3 in test CG3), due to the fact that their saturation and, consequently, their swelling, was higher. Due to this density decrease, the degrees of saturation were lower than what could be expected by the high water content. In fact, degrees of saturation higher than 90% were only reached in the 3 cm closest to the hydration surface after 6 months of TH treatment, in 8 cm after 12 months, in 10 cm after 24 months and in 25 cm in the 7.6-year test. Taking a value of 1 g/cm^3 for the density of the adsorbed water, the 10 cm of bentonite closest to the hydration surface in test CG3 would be fully saturated. On the other hand, near the heater (18 cm) the densities remain the same from 6 to 24 months, and the degrees of saturation decrease from the initial 55-60% to values around 25% in the vicinity of the heater.

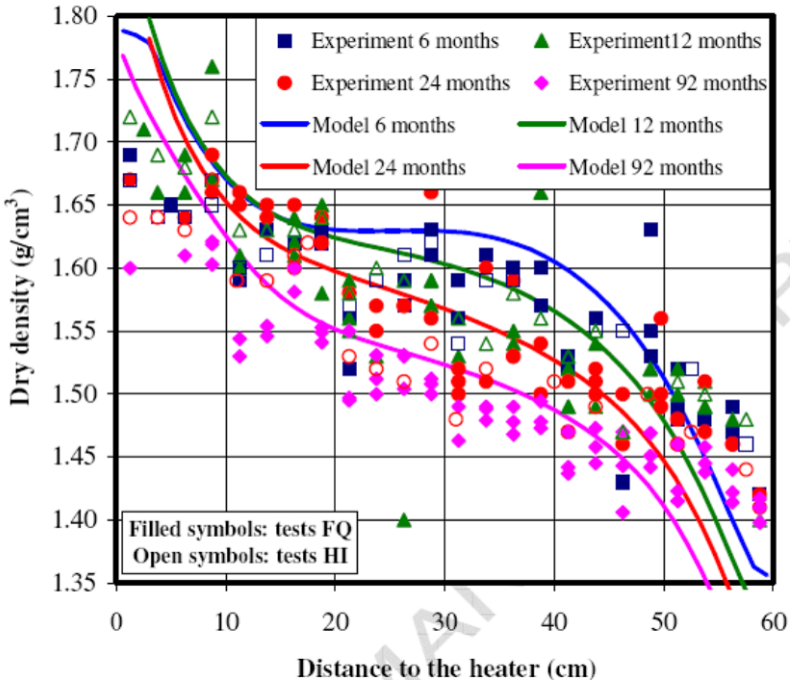

Fig. 12 Final dry densities along the bentonite columns of the different tests: experimental and modeling results.

There is also an overall decrease of the average density of the bentonite, which is much more significant in the 7.6-year test. This is attributed to the deformation of the Teflon walls of the cell caused by the swelling of the bentonite, which increased over time, and also to the further expansion of the bentonite on dismantling of the cells and to the trimming of subsamples, which may cause their density to decrease. These last reasons may cause the dry densities and degrees of saturation given above to be fictitiously lower than the actual ones.

Considering the uncertainties, comparison with modeling shows quite good agreements. The model is able to capture qualitatively and quantitatively the main trends of the experiments. The main disparity between model and results is found in the zone closest to the hydration front, especially in the longest tests. This can be caused by the unavoidable drying during sampling of the sections whose water content is extremely high, what would make the water content and dry density measured lower and higher, respectively, than the actual ones.

Thus, the modeling of the heating and hydration of the cells has demonstrated the capability of the formulation and computer code to model the complex behavior of expansive clays submitted to coupled THM actions.

As it has been explained in the previous sections, the water intake at the end of the tests can be deduced from three different measurements. The most direct ones are the online measurement performed during the tests by the volume change apparatuses, and the weighing of the column at the end of the tests, that allows computing the water mass taken by comparison with the initial weight of the columns. Both methods are subject to error. The first one because the equipments used to measure online during such long periods of time can suffer failures and leaks, and the second one, because the extraction of the bentonite from the cells is difficult and some material can be lost during the process. This is the reason why there are not final weight values for tests FQ1/2 and HI1. An additional method to determine the water intake would be to compute it from the average water content measured in the different sections.

A comparison of the values obtained with the three methods is given in Fig. 13. Despite several problems, due to various failures of the equipments, the final water contents

calculated from the online water intake measurements agree quite well with the water contents calculated at the end of the tests by the other two methods. Furthermore, the coincidence between the water intakes measured by the volume change apparatuses and those measured at the end of the tests by final and initial weight differences and those determined by direct measurement in the different sections, allows to state that the cells have remained watertight during operation. The coherence among values gives confidence on the results obtained and allows determining their possible range of variation. In addition, the agreement between model results and measurements is quite good.

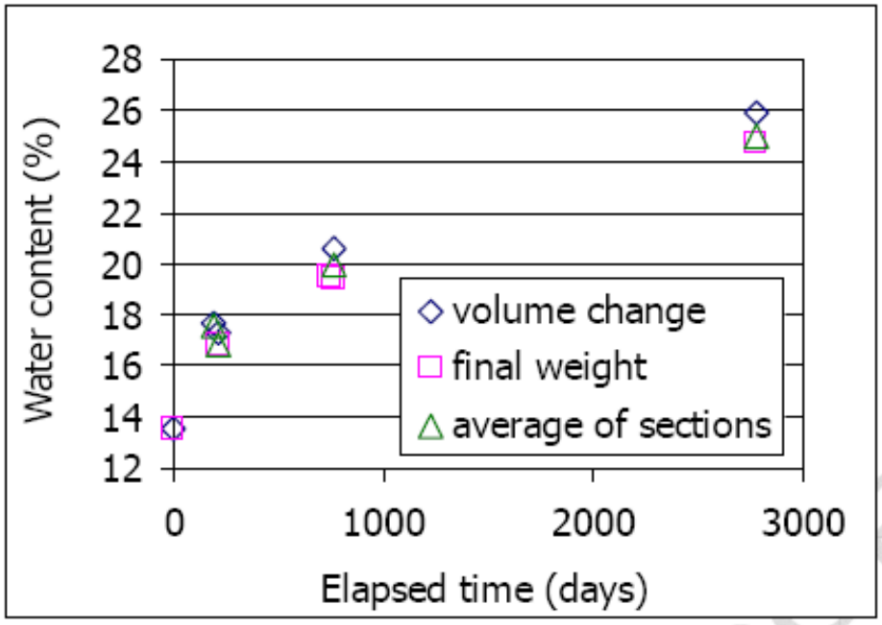

Fig. 13 Water content at the end of the TH tests according to different measurements.

ii) LAGAMINE

With the given parameters, the simulations of experimental process are carried out. The evolution of temperature vs. time in the lateral direction (along the red line) is illustrated in Fig. 14. As defined in boundary conditions, the temperature is kept at 90 °C on the nodes connected to the electric heater. At the beginning, the temperature of compacted bentonite increases rapidly, especially in the first month. Thanks to the frontier thermal elements, the temperature on the exterior boundary also increases with time.

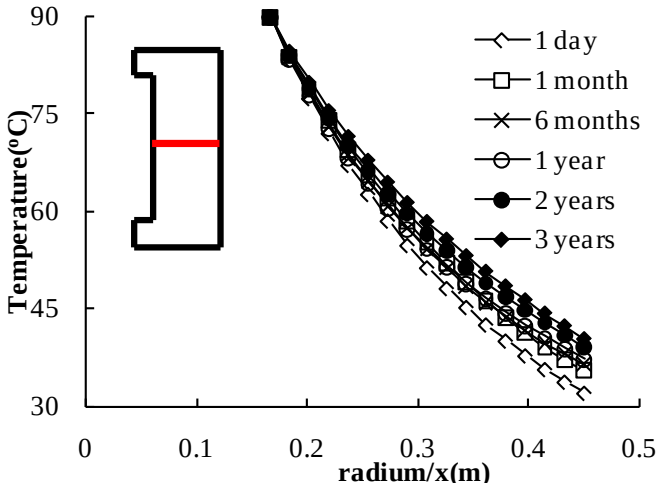

Fig. 14 Evolutions of temperature vs. time (along the red line).

The compacted bentonite is progressively saturated by the water inflow (Fig. 15), which is in an opposite direction to heat flow. However, due to the extremely low permeability and evaporation, the compacted bentonite close to the heater still stays partially saturated after 3 years (Fig. 16).

Fig. 15 Water flow at the end of simulation (3 years).

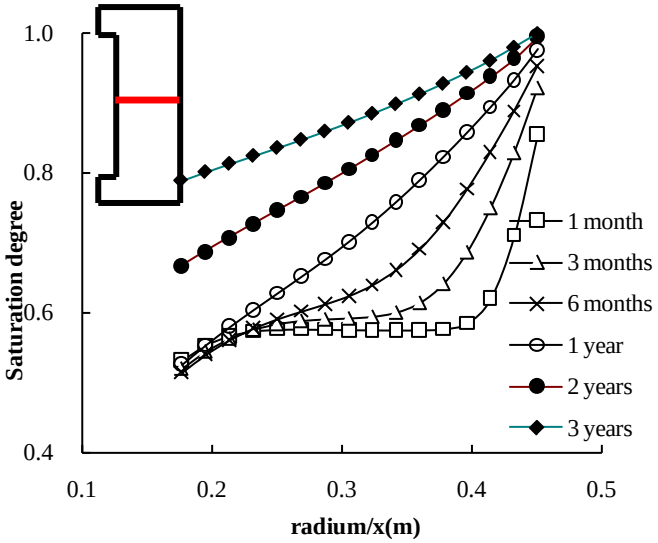

Fig. 16 Distribution of saturation degree with time.

In terms of suction, due to the saturation process by water penetration, the suction is decreased globally (Fig. 17). It is interesting that a more significant suction (100 MPa) than the initial value (80 MPa) can be noticed at the beginning. It indicates that the bentonite is desaturated in this period of time.

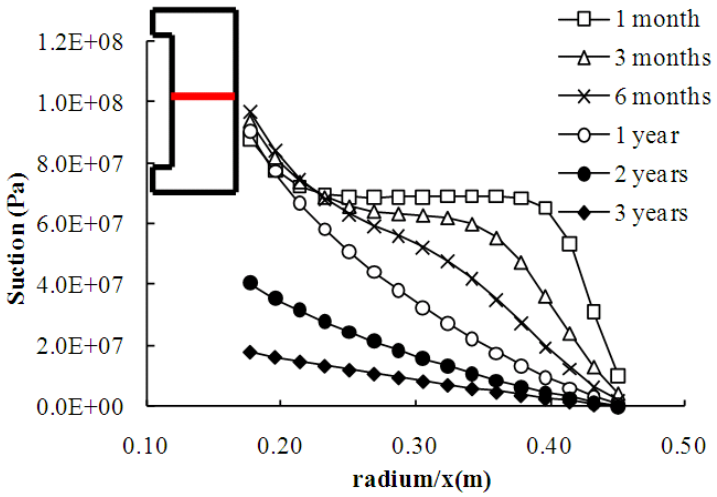

Fig. 17 Suction-time evolution in lateral direction.

This phenomenon is well presented in Fig. 18, in which the suction responses of the three points (A, B, C) in lateral direction are illustrated. It is noticed that at point A, the suction

increases at first, and then decreases. This desaturation-saturation process can be attributed to the evaporation phenomenon generated by high temperature of the electrical heater. In Fig. 19, water vapor is generated and transported towards outer boundary in the field exposed to high temperature. The desaturation process indicates that at the beginning, the evaporation phenomenon is dominant compared to the saturation effect induced by the water inflow. This phenomenon is also observed in other experimental tests, like the Canister Retrieval Test (CRT) carried out by SKB (Akesson et al., 2010).

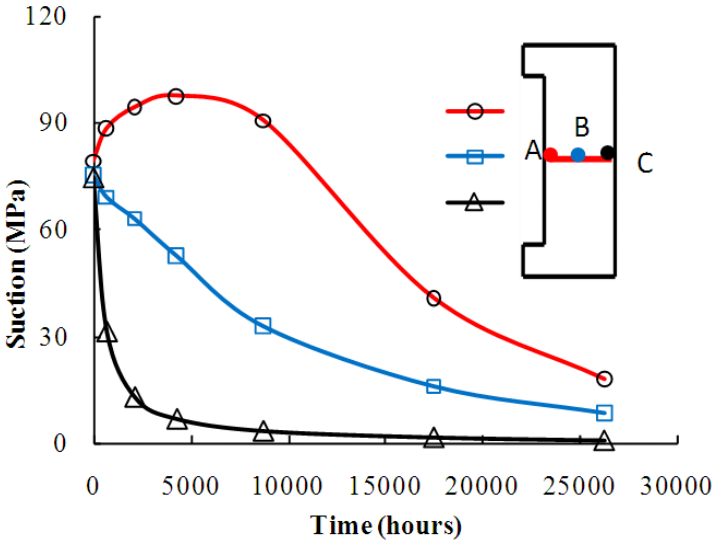

Fig. 18 Suction responses of the three points in lateral direction.

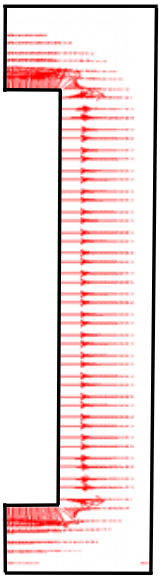

Fig. 19 Vapor flows at the end of simulations (3 years).

The predicted water pressure with time is illustrated in Fig. 20. It is noticed that in the field exposed to high temperature, the suction is more significant, especially for the area close to the upper surface and the bottom of the electrical heater. At the end of the simulations (3 years), a suction of around 59 MPa is reached in this field. This result seems reasonable considering that the field is far from the outer boundary. Moreover, the evaporation generated by high temperature is also more significant.

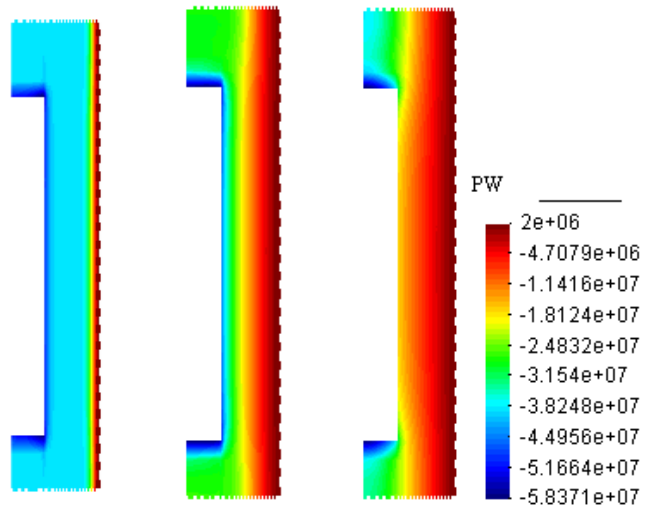

(a) 1 months. (b) 1 year. (c) 3 years.

Fig. 20 Distribution of water pressure.

The swelling pressure variation with time at point A with co-ordinates r=0.15 m and z=0.123 m is illustrated in Fig. 21.

It can be noticed that the swelling pressure increases rapidly at the beginning, and a value of 1.5 MPa is obtained after 3 years, which seems relatively limited. It can be attributed to two reasons: first, considering the saturation process is not completed, the maximum value is not yet reached; on the other hand, the expansion strain induced by the variation in microstructure of bentonite during wetting process is not considered in the BBM model.

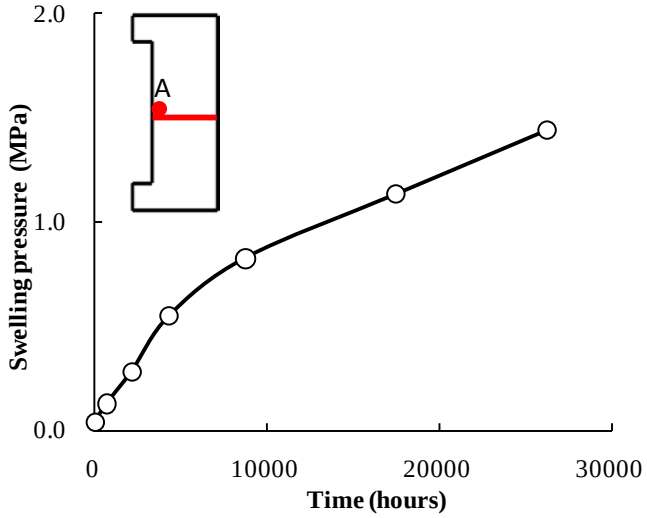

Fig. 21 Swelling pressure evolution at point A.

6. Summary and conclusions

i) CODE_BRIGHT

The conditions of the bentonite in an engineered barrier for HLW disposal have been simulated experimentally in a series of tests. Columns of compacted bentonite kept in hermetic Teflon cells were hydrated with low-salinity granitic water at the upper surface while they were heated at the bottom surface at a temperature of 100^{o}C during different periods of time. The columns consisted of six stacked compacted blocks of 7 cm in diameter and 10 cm high. Consequently, the total length of clay inside the cells was 60 cm, the same as the thickness of the bentonite barrier in the mock-up test of the FEBEX Project (ENRESA, 2006). The initial average dry density of the bentonite was 1.66 g/cm^3 and the water content 13.6%. The duration of the tests was 6, 12, 24 and 92 months. The temperatures inside the clay and the water intake were satisfactorily measured during the tests and, at the end, the cells were dismantled and the dry density and water content were determined in different positions along the blocks. The online measurements and the results of the postmortem tests performed in the bentonite after dismantling have been reported in the paper. In addition, the tests have been modeled as a boundary value problem using a numerical code especially developed to handle coupled THM problems in porous media, and the model results have been compared with the experimental measurements. The following conclusions can be

drawn:

(1) There is a sharp temperature gradient in the vicinity of the heater. The temperatures inside the clay during the TH treatment are slightly lower as the duration of the test is longer, what is due to the increase in thermal conductivity of the clay with water content and the higher heat dissipation of the clay as it becomes wetter.

(2) At the end of all the tests there were important water content and dry density gradients along the bentonite column. The increase in water content caused by hydration is linked to a reduction in dry density as a consequence of swelling, whereas the decrease of water content caused by evaporation near the heater is linked to an increase of dry density as a consequence of shrinkage.

(3) The density and water content gradients will condition temporarily the hydro-mechanical properties of the bentonite that are dependent on both, as the permeability and the swelling capacity (Villar et al., 2005a, 2008).

(4) Hydration and heating caused also geochemical modifications that are described elsewhere (Villar et al., 2008), in particular dissolution of some mineral species of the bentonite and movement of soluble ions by advection. The movement of some ions was affected by mineral equilibrium reactions (dissolution/precipitation) and exchange reactions, what gave place also to modification of the exchangeable cation complex. However, no major mineralogical changes were detected.

(5) The final average degree of saturation in the longest test (7.6 years), considering a water density of 1 g/cm^3, is 92%, what highlights the slowness of the hydration process of compacted bentonite. The joints between blocks become sealed much before the water content is close to saturation.

(6) The numerical model used can reproduce the global trends observed in the tests, both the results related to the evolution of the main variables of the tests and those related to the postmortem study. Most of the constitutive model and parameters assumed in the analysis presented here were developed and obtained from laboratory tests carried out during the FEBEX project and they are the same ones adopted for the main analysis of the large-scale heating tests of the FEBEX project (i.e. mock-up and in situ tests, ENRESA, 2006). The possibility to model properly heating tests at different scales with a unique set of parameters points to an appropriate selection of the processes and parameters.

(7) Indeed, there is still room for improvements and further developments are required. However, it is believed that the formulation provides a suitable platform for further advances and enhanced understanding. In fact, the consideration of the interactions between the two basic pore levels (macro and micropores) that exist in expansive clay was later on included in the model (Lloret et al., 2003), as well as the possible effect of the existence of a threshold hydraulic gradient on the hydraulic response of the barrier (Sanchez et al., 2007b) and of the impact of temperature on the hydro-mechanical properties of the bentonite (Sanchez et al., 2007a).

(8) Tests like those presented in this work, in which the expansive clay and the THM conditions are very similar to the ones expected in large-scale tests, are very useful for a better understanding of the behavior of expansive clays under controlled thermal and hydraulic gradients similar to those expected in a HLW repository. This kind of experiments is also very useful for the validation of mathematical formulations and computer code.

ii) LAGAMINE

The buffer material is one of the main engineered barriers for the HLW repository. In order to study the behavior of the compacted GMZ-Na-bentonite under coupled THMC conditions, a large-scale mock-up facility, China-Mock-up based on a preliminary concept of HLW repository in China, has been designed and constructed in the laboratory of BRIUG.

The current experimental data is presented in the report, including the variation of temperature, relative humidity, stress and displacement etc. A thermo-hydro-mechanical model is proposed to reproduce the complex coupling behavior of the compacted GMZ bentonite. With the proposed model, numerical simulation of the China-mock-up test is realized. According to the analysis of the experimental and numerical results, some conclusions are obtained and summarized as follows:

(1) The experimental data indicates that the saturation process of the compacted bentonite is strongly influenced by the competitive mechanism between the drying effect induced by the high temperature and the wetting effect by the water penetration from the outer boundary. For this reason, the desiccation phenomenon is observed in the zone close to the heater.

(2) Due to the THM coupling phenomena and its influence to the mechanical behavior of the compacted bentonite, the heater is not stationary in the facility. At present, an upward movement of the heater is observed.

(3) Based on the qualitative analysis of the predictive results, it is suggested that the proposed model is capable to reproduce the principal coupled THM behavior of the compacted GMZ bentonite. As a qualitative analysis of the predictive results, the numerical study realized only can be considered as a preliminary verification of the proposed model. With the progress of the experimental test, further study is needed.

The China-Mock-Up experiment is an important milestone of the buffer material study for HLW disposal in China. The observed THMC processes taking place in the compacted bentonite-buffer during the early phase of HLW disposal can provide a reliable database for numerical modeling and further investigations of EBS, and the design of HLW repository.

7. References

Akesson M, Borgesson L, Kristensson O., 2010. THM modeling of buffer, backfill and other system components: critical processes and scenarios. Stockholm: SKB technical report.

Alonso E E, Gens A, Josa A., 1990. A constitutive model for partially saturated soils. Géotechnique, 40 (3): 405–430.

Alonso E E, Vaunat J, Gens A., 1999. Modelling the mechanical behavior of expansive clays. Engineering Geology, 54 (1): 173–183.

Chen, B., Qian, L.X., Ye, W.M., Cui, Y.J. & Wang, J. 2006. Soil-water characteristic curves of Gaomiaozi bentonite. *Chinese Journal of Rock Mechanics and Engineering*, 25 (4): 1054-1058.

Charlier R., 1987. Approach unifiée de quelques problèmes non linéqires de mécanique des milieux continus par la méthode des éléments finis. Ph.D. Thesis. Liège: Université de Liège.

Collin F, Li X L, Radu J P, Charlier R. 1999. Thermo-hydro-mechanical coupling in clay barriers. Engineering Geology, 54 (2/3): 173–183.

Cui Y J, Tang A, Quian L X, Ye W M, Chen B., 2011. Thermal-mechanical behavior of Compacted GMZ bentonite. Soils and Foundations, 51 (6): 1065–1074.

ENRESA, 2006. Full-scale Engineered Barriers Experiment. Updated Final Report 1994 – 2004. Publicación Técnica ENRESA 05-0/2006, Madrid, 590pp.

Gens, A., Guimarães, L. do N., Olivella, S. & Sánchez, M. 2010. Modelling thermo-hydro-mechano-chemical interactions for nuclear waste disposal. *Journal of Rock Mechanics and Geotechnical Engineering*. 2010, 2 (2): 97-102.

Karnland, O., Sandén T., Johannesson Lars-Erik, et al. 2000. *Long term experiment of buffer material, Final report on the pilot parcels*, SKB Technical Report, TR-00-22.

Li, X. L., Frédéric, B & Johan, B. 2006. The Belgian HLW repository design and associated R&D on the THM behaviour of the host rock and EBS. *Chinese Journal of Rock Mechanics and Engineering*, 2006, 25 (4): 682-692.

Li, X. L., Bastiaens, P., VanMarcke, P, et al. 2010. Design and development of large-scale in-situ PRACLAY heater experiment and horizontal high-level radioactive waste disposal gallery seal experiment in Belgian HADES. *Journal of Rock Mechanics and Geotechnical Engineering*. 2010, 2 (2): 103–110.

Lloret, A., Villar, M.V., Sánchez, M., Gens, A., Pintado, X., Alonso, E., 2003. Mechanical behaviour of heavily compacted bentonite under high suction changes. Géotechnique 53 (1), 27 – 40.

Lloret, A., Romero, E., Villar, M.V., 2004. FEBEX II Project Final report on thermo-hydro-mechanical laboratory tests. Publicación Técnica ENRESA 10/04, Madrid,180pp.

Lloret, A. & Villar, M.V. 2007. Advances on the knowledge of the thermo-hydro-mechanical behaviour of heavily compacted "FEBEX" bentonite. *Physics and Chemistry of the Earth*. 2007, 32: 701-715.

Liu, Y.M., Wen, Z.J., 2003. Study on clay-based materials for the repository of high level radioactive waste. *Journal of Mineralogy And Petrology*, 2003, 23(4): 42-45. (in Chinese)

Liu, Y.M., Cai M.F., Wang J., 2007a. Compressibility of buffer material for HLW disposal in China. *Uranium Geology*, 23, 91-95. (in Chinese)

Liu, Y.M., Cai M.F., 2007b. Thermal conductivity of buffer material for high-level waste diaposal. Chinese Journal of Rock Mechanics and Engineering 26(S1), 3891-3896. (in Chinese)

Olivella, S., Gens, A., Carrera, J., Alonso, E.E., 1994. Nonisothermal multiphase flow of brine and gas through saline media. Transport in Porous Media 15, 271 – 293.

Olivella, S., Gens, A., Carrera, J., Alonso, E.E., 1996. Numerical formulation for a simulator (CODE-BRIGHT) for the coupled analysis of saline media. Engineering Computations 13 (7), 87 – 112.

Olivella, S., Gens, A., 2000. Vapour transport in low permeability unsaturated soils with capillary effects. Transport in Porous Media 40, 219 – 241.

Pacovsky J., Svoboda J. & Zapletal L., 2007. Saturation development in the bentonite barrier of the Mock-Up-CZ geotechnical experiment. *Physics and Chemistry of the Earth*, 32(2007), 767-779.

Philip J R, de Vries D A. 1957.Moisture movement in porous materials under temperature gradients. Transactions, American Geophysical Union, , 38 (2): 222–232.

Pintado, X., Ledesma, A., Lloret, A., 2002. Backanalysis of thermohydraulic bentonite properties from laboratory tests. Engineering Geology 64, 91 – 115.

Romero, E., Li, X. L. 2006. Thermo-hydro-mechanical characterization of OPHELIE backfill mixture. *Chinese Journal of Rock Mechanics and Engineering*, 2006, 25 (4): 733-740.

Sánchez, M., Gens, A., 2006. FEBEX Project final report. Final report on thermo-hydro- mechanical modelling. Publicación Técnica ENRESA 05-2/2006, Madrid, 163pp.

Sánchez, M., Villar, M.V., Gens, A., Olivella, S., Guimar 鉚 s, L., do, N., 2007a. Modelling the effect of temperature on unsaturated swelling clays. In: Proc Int Symp on Numerical Models in Geomechanics (NUMOG X), Rhodes, April, 2007.

Sánchez, M., Villar, M.V., Lloret, A., Gens, A., 2007b. Analysis of the expansive clay hydration under low hydraulic gradient. In: Experimental Unsaturated Soil Mechanics. Springer Proceedings in Physics, vol. 112. Springer, Berlin, pp. 309–318.

Tang A M, Cui Y J., 2009. Modelling the thermo-mechanical volume change behaviour of compacted expansive clays. Geotechnique, 59 (3): 185–195.

Villar, M.V., Martín, P.L., Barcala, J.M., 2005a. Modification of physical, mechanical and hydraulic properties of bentonite by thermo-hydraulic gradients. Engineering Geology 81, 284–297.

Villar, M.V., Sánchez, M., Lloret, A., Gens, A., Romero, E., 2005b. Experimental and numerical study of the THM behaviour of compacted FEBEX bentonite in smallscale tests. In: Alonso, E.E., Ledesma, A. (Eds.), Advances in Understanding Engineered Clay Barriers. A.A. Balkema Publishers, Leiden, pp. 323–335.

Villar, M.V., Fernández, A.M., Martín, P.L., Barcala, J.M., Gómez-Espina, R., Rivas, P., 2008. Effect of heating/hydration on compacted bentonite: tests in 60-cm long cells. Colección Documentos CIEMAT, Madrid, 72pp.

Wang, J. 2010. High-level radioactive waste disposal in China: update 2010. *Journal of Rock Mechanics and Geotechnical Engineering*, 2010, 2 (1): 1–11.

Ye, W.M., Schanz, T., Qian, L.X.,Wang. J., 2007. Characteristics of swelling pressure of densely compacted gaomiaozi bentonite GMZ01. Chinese Journal of Rock Mechanics and Engineering, 26(S2), 3861-3865.(in Chinese)

Ye, W.M., Cui, Y.J., Qian L.X. & Chen, B., 2009a. An experimental study of the water transfer through confined compacted GMZ-bentonite. *Engineering Geology*, 108(3-4): 169-176.

Ye, W.M., Wan, M., Chen, B., 2009b. Effect of temperature on soil-water characteristics and hysteresis of compacted Gaomiaozi bentonite. Journal of Central South University Technology 16, 821-826.